Fluorinated γ-alumina aerogels and xerogels: characterisation and catalytic behaviour

Tomaž Skapin [1]

Department of Inorganic Chemistry and Technology, "Jožef Stefan" Institute, Jamova 39, 1001 Ljubljana, Slovenia

and

Erhard Kemnitz

Institute of Chemistry, Humboldt University, Hessische Strasse 1/2, D-10115 Berlin, Germany

Received 22 February 1996; accepted 16 April 1996

The porosity of γ-alumina-based materials is an important parameter affecting the extent of fluorination (aerogels > commercial γ-Al_2O_3 > xerogels) and, consequently, also the textural, acidic and catalytic properties of the final fluorinated materials. Only the highly fluorinated aluminas having strong Lewis acidic sites catalyse the isomerisation of CHF_2CHF_2 to CF_3CH_2F.

Keywords: γ-alumina; aerogel; xerogel; fluorination; acidity; texture; catalytic activity; isomerisation of CHF_2CHF_2

1. Introduction

Recently it was demonstrated that chromium-doped alumina aerogels can be used as starting materials for the preparation of highly porous fluoride materials [1] which could find use as catalysts for vapour phase reactions involving halogenated lower hydrocarbons. In the present study the results of characterisation of fluorinated pure alumina aerogels are presented. To determine the influence of the initial porosity on the properties of the fluorinated materials, aerogels were compared to less-porous xerogels and intermediately-porous commercial γ-Al_2O_3. Catalytic activity was, in addition to other model reactions (dehydrochlorination of CCl_3CH_3 and isomerisation of 1-butene), checked in CHF_2CHF_2 isomerisation. This reaction presents one of the possible routes to the technically important CF_3CH_2F (HFC-134a). In the patent literature chromia- [2], as well as alumina-derived materials [3], are claimed to be active catalysts for this reaction. The kinetic and mechanistic aspects of CHF_2CHF_2 isomerisation over a chromia catalyst were investigated recently [4].

2. Experimental

Catalyst preparation. In the first step pellets were extruded from gelatinous precipitates obtained by the addition of ammonia to the solution of aluminium chloride. Each batch of pellets was divided in two equivalent portions: the first portion was transformed to xerogel (X-samples) by ordinary oven-drying at 120°C, the second part was converted to the aerogel (A-samples) by the supercritical drying procedure as previously described [1]. The commercial γ-alumina (C-samples) was in the form of pellets with nominal diameter of 0.8 mm (Shell S-618). Before fluorination all materials were pre-treated by calcining in a flow of air at 450°C. Fluorination was performed with pure trifluoromethane (CHF_3) or with HF diluted to 20 vol% with nitrogen. The quantity of the fluorinating agent used was always in large excess to that required for complete fluorination. Denomination of samples and some preparation conditions are given in table 1.

Characterisation. Bulk crystalline phases were identified from X-ray diffraction (XRD) patterns (Philips PW 1710 diffractometer, Cu-Kα radiation). Nitrogen physisorption results were obtained at liquid nitrogen temperature (Micromeritics ASAP 2000 instrument). Photoacoustic (PA) spectra of pyridine, adsorbed at 150°C, and temperature-programmed desorption (TPD) of ammonia, adsorbed at 100°C, were performed as previously described [5]. Morphology and texture were analysed by scanning electron microscopy (SEM) (Jeol JXA 840). Fluoride content was determined after total decomposition with an ion-selective electrode [6].

Catalytic reactions. Dehydrochlorination of CCl_3CH_3 to $CCl_2{=}CH_2$ at 130°C and isomerisation of 1-butene to cis/trans-2-butene at 200°C were carried out

[1] To whom correspondence should be addressed.

Table 1
Preparation conditions and composition of materials

Sample	Fluorinating agent	Temperature [a] (°C)	Fluorine content (% F^-)	XRD detected phases (by priority)
A [b]	–	320	–	boehmite
A450	–	450 [c]	–	γ-Al_2O_3, boehmite
A-H350	HF/N_2	350	67.1	α-AlF_3, β-AlF_3
A-F300	CHF_3	300	43.3	γ-Al_2O_3, α-AlF_3
A-F350	CHF_3	350	61.1	α-AlF_3, β-AlF_3
A-F400	CHF_3	400	66.1	α-AlF_3
X450	–	450 [c]	–	γ-Al_2O_3
X-H350	HF/N_2	350	38.5	γ-Al_2O_3, α-AlF_3
X-F350	CHF_3	350	37.3	γ-Al_2O_3, α-AlF_3
C	–	–	–	γ-Al_2O_3 [d]
C-H350	HF/N_2	350	46.1	γ-Al_2O_3, α-AlF_3
C-H450	HF/N_2	450	63.6	α-AlF_3
C-F480	CHF_3	480	64.7	α-AlF_3

[a] Maximum temperature in the specific preparation step.
[b] Sample after supercritical drying.
[c] Calcined in flow of air.
[d] As specified by the manufacturer.

under continuous gas flow conditions [7]. Isomerisation of CHF_2CHF_2 was investigated by the pulse technique [4], using each sample of a catalyst in a continuous experiment, first at 400°C and then at 450°C. The amount of catalyst used was 0.24–0.43 g for aerogels and 0.9–1.3 g for xerogels and commercial γ-Al_2O_3, and the resulting residence times were 65 ± 5 s. Analyses of the reaction products from all test reactions were performed with gas chromatography (Shimadzu GC-14A).

3. Results and discussion

3.1. Fluorination of the oxide materials

An increase in the surface area accompanied by a reduction in volume of pores determined by nitrogen adsorption (samples A and A450 in table 2) were observed after heating the boehmite aerogel to 450°C. These changes are due to the conversion of the poorly crystallised boehmite to almost amorphous γ-Al_2O_3 [1] which has two effects: an increase in the porosity below 10 nm and a partial collapse of the fragile aerogel network that reduces the volume of pores larger than 10 nm. The asymmetric distribution of pores for the γ-Al_2O_3 aerogel is shown in fig. 1a. In contrast, the oxide xerogel exhibits much lower volume of pores with a narrow size distribution in the range 2–7 nm (fig. 1b). The textural properties of the commercial γ-Al_2O_3 lie between the properties of aerogel and xerogel (fig. 1c). The most evident difference between the starting oxide materials is in the porosity with aerogel and xerogel representing the two extremes.

Chemical analysis showed a large degree of fluorine

Table 2
Nitrogen physisorption results

Sample	a_s(BET) (m^2/g)	$V_{p(N_2)}$ (cm^3/g)	$\langle d_p \rangle$ [a] (nm)	Type of hysteresis loop [b]
A	273.5	1.507	22.0	H1/H3
A450	388.0	1.314	13.5	H1/H3
A-H350	31.6	0.117	14.8	H1/H3
A-F300	150.4	0.708	18.8	H1/H3
A-F350	40.7	0.134	13.2	H1/H3
A-F400	9.8	0.038	15.3	H1/H3
X450	252.1	0.283	4.5	H2
X-H350	34.2	0.126	14.7	H1/H2
X-F350	33.0	0.126	15.3	H1/H2
C	223.6	0.689	12.3	H2
C-H350	71.0	0.371	20.9	H1/H2
C-H450	20.3	0.095	18.8	H1/H3
C-F480	22.1	0.178	32.1	H1/H3

[a] Average cylindrical pore diameter, $\langle d_p \rangle$; $\langle d_p \rangle = 4V_{p(N_2)}/a_s(\text{BET})$.
[b] Type of hysteresis loop at low/high relative pressure according to the classification in ref. [12].

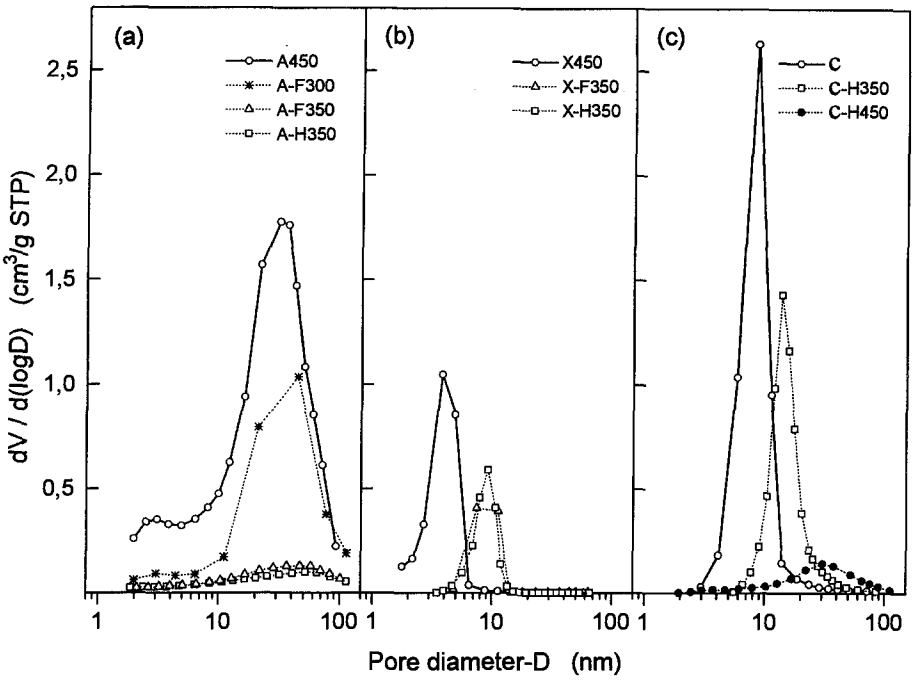

Fig. 1. Pore size distribution for: (a) aerogels, (b) xerogels and (c) commercial γ-Al_2O_3; starting oxides (solid lines), fluorinated materials (dotted lines).

incorporation for all samples after fluorination with either CHF_3 or HF (table 1). The results obtained with CHF_3 are only slightly lower than those obtained with HF, although it was claimed that considerable fluorination of γ-Al_2O_3 with CHF_3 takes place at temperatures above 400°C [8]. The great influence of the temperature on the degree of fluorination is evident when comparing the fluorination experiments at different temperatures (table 1). Additionally, due to the differences in surface area and especially the porosity of the different oxides used, the extent of fluorination varied largely as the textural properties. At 350°C oxide aerogels were, in contrast to xerogels and commercial γ-Al_2O_3, almost completely transformed (90–99%) to aluminium trifluoride (AlF_3), as calculated from the fluorine content. XRD results are consistent with the chemical analysis (table 1). In highly fluorinated samples well-crystallised α-AlF_3 was the main phase, and a small amount of the metastable β-AlF_3 could also be observed in aerogels fluorinated at 350°C. Although the samples with lower degrees of fluorination also exhibited relatively high AlF_3 contents in the range 55–68%, the XRD patterns were those of unreacted γ-Al_2O_3 with some peaks that could be related to the beginning of the formation of crystalline AlF_3 phases. It is obvious that even at this stage of fluorination the fluoride phase is still highly dispersed and in the form of very small crystallites that could barely be detected by XRD [9,10].

Depending on the extent of fluorination, surface area and pore volume are reduced and pore diameter is increased (table 2) in accordance with previous investigations [1,8,9,11]. For the aerogels fluorinated at 350°C the volume of all pores is strongly reduced, but the remaining pores still show a very broad distribution over the entire 2–100 nm range (fig. 1a). The pore size distribution of the A-F300 sample (fig. 1a) shows that at the beginning of fluorination the smaller pores are affected first, probably by combined pore filling and plugging processes, and then further fluorination reduces the 10–100 nm pores, since extensive crystallisation and homogeneous collapse of the original aerogel network take place due to the uniform densification on the microscale [1]. Fluorinated xerogels and commercial γ-Al_2O_3 samples preserved the relatively narrow pore size distribution and showed typical pore volume decrease and pore diameter increase (figs. 1b and 1c). At high temperatures of fluorination the broad pore size distribution characteristic of aerogels is also obtained for commercial γ-Al_2O_3 (fig. 1c).

SEM micrographs, presented in fig. 2, are in complete accordance with the textural properties already discussed. Aerogel (fig. 2a) is in the form of a very open network consisting of weakly interconnected aggregated particles and crystals of different sizes and shapes. Pores in the range 2–100 nm are situated between the particles/crystals that form the aggregates and represent only a small part of the whole porosity. The majority of pores are related to very large pores (or channels) between the aggregates (fig. 3a) and cannot be detected by nitrogen adsorption. Xerogels (figs. 2b and 2c) have a much more dense and homogeneous structure. The void spaces between almost spherical particles are uniform, which explains the narrow pore size distribution observed for these samples. The exterior of xerogel pellets (fig. 2b)

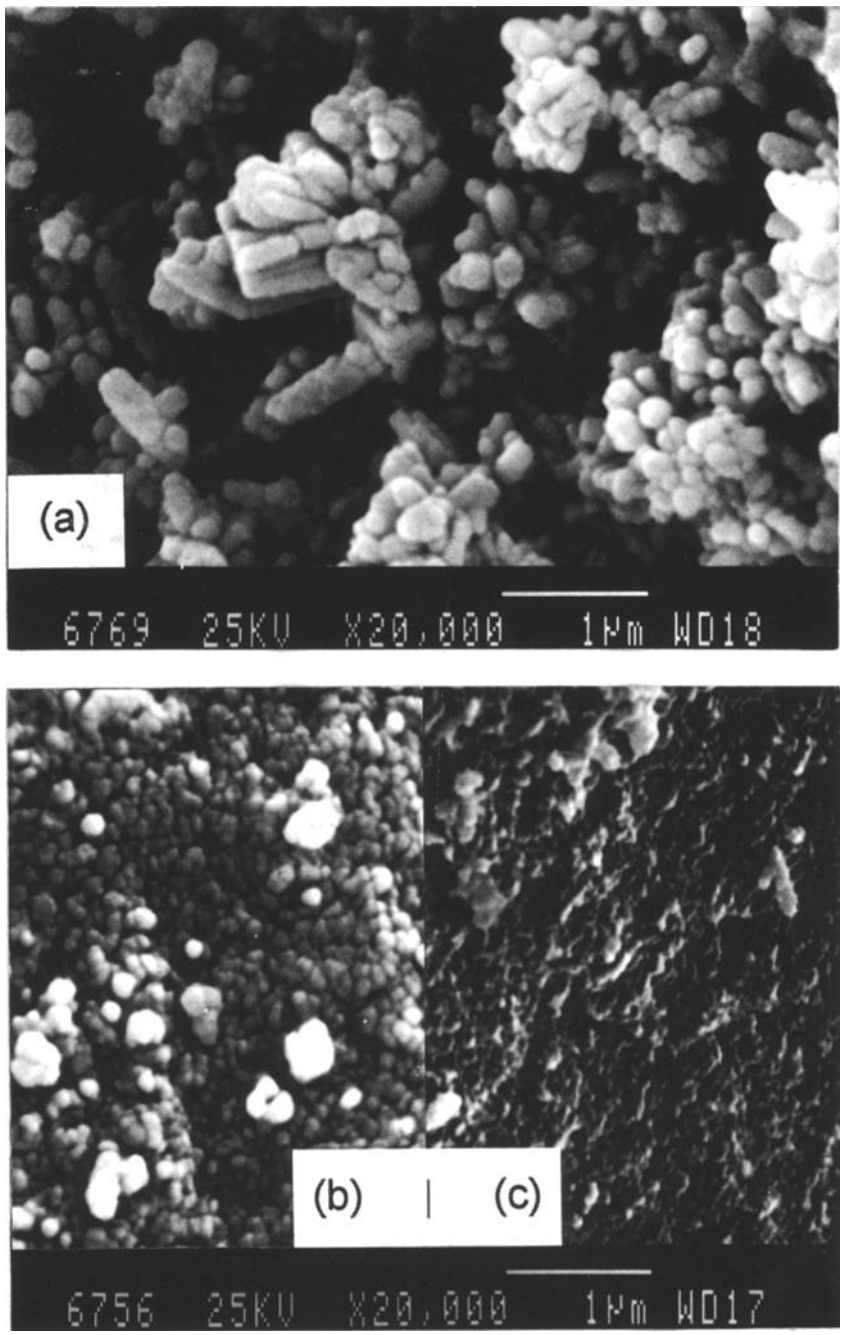

Fig. 2. SEM micrographs of samples fluorinated with HF at 350°C: (a) aerogel, (b) xerogel (surface) and (c) xerogel (interior); magnification 20000×.

shows larger particles than the interior (fig. 2c). The formation of larger particles on the surface can block some of the pores, thus hampering the fluorination of the interior. This may be one of the reasons for the low degree of fluorination in xerogels. It is worth mentioning that the nitrogen isotherms for aerogels and xerogels, typical of aggregates or more rigidly joined agglomerates [12] respectively, are in accordance with the morphology observed.

3.2. Surface characterisation

Characterisation of surface acidity was achieved in two ways: PA spectroscopy of adsorbed pyridine and ammonia TPD to differentiate between type, number and strength of the acidic sites, then dehydrochlorination of CCl_3CH_3 and isomerisation of 1-butene, the two reactions known to proceed on Lewis [13,14] or Brønsted [15,16] acid sites respectively.

The PA spectra of adsorbed pyridine are in a good

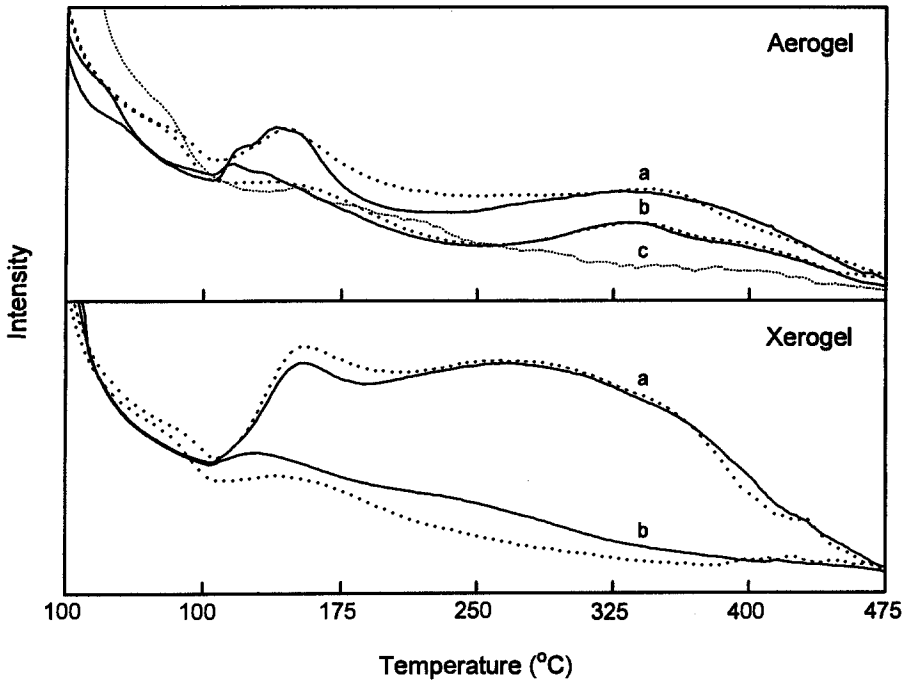

Fig. 3. Ammonia TPD profiles for aerogels and xerogels fluorinated at 350°C; (a) first run, (b) second run, (c) first run for the aerogel additionally fluorinated with HF at 550°C; samples fluorinated with CHF_3 (solid lines) and HF (dotted lines).

agreement with the results obtained in earlier work [5]. The nature of the surface acidic sites after fluorination of oxide precursors is dictated by the extent of fluorine incorporation and is therefore directly related to the temperature of fluorination and/or porosity of the oxide. For all fluorinated samples a shift of the peak at 1444 cm^{-1}, characteristic for the Lewis acid sites in γ-Al_2O_3 materials, to 1453 cm^{-1} is observed as the result of the strengthening of the Lewis centres due to fluorination [5]. Some Brønsted acidity is also present on highly fluorinated samples, as indicated by the intensity of the 1492 cm^{-1} peak which originates from pyridine adsorbed on Lewis and Brønsted acid centres. Surface species that from Brønsted acid centres on such samples are easily removed by evacuation at 150°C. The result is a large reduction in the intensity of the 1492 cm^{-1} peak with the 1453 cm^{-1} peak practically unchanged. Lower fluorinated samples exhibit much higher Brønsted acidity with very intense 1492 cm^{-1} peaks and with the appearance of peaks at 1542 cm^{-1}. The latter are characteristic exclusively of pyridine adsorbed on Brønsted acid centres.

The first-run ammonia TPD profiles for xerogels (fig. 3) suggest the presence of numerous acid sites with a very broad distribution of strengths. The PA spectra are consistent with this, indicating the presence of Lewis and Brønsted acid centres. Parallel to ammonia, water is also desorbed from xerogels showing very similar broad desorption profiles. In the second run the TPD intensities are considerably reduced. The water released in the first run probably originated from condensation reactions of surface hydroxyl groups, dramatically affecting the number and the strength of all acidic sites. Similar TPD profiles were observed for commercial γ-Al_2O_3 fluorinated at 350°C with the exception of the second run where a low intensity desorption maximum was noticed at approximately 330°C. In contrast, first-run TPD profiles for aerogels show two distinctive maxima and are remarkably similar to the profiles obtained from a pure β-AlF_3 phase [5]. This suggests that the profiles for these samples are the result of the presence of this phase, since α-AlF_3 shows no ammonia desorption [5]. After treating in a flow of HF at 550°C that resulted in a β- to α-AlF_3 conversion, a TPD profile with no desorption (fig. 3c) in the range of 250–475°C was obtained. The most important feature of the second-run TPD profiles for aerogels is that the high temperature maximum at approximately 335°C is still observed, indicating the presence of strong acidic sites which are only partly affected by the water released in the first run. Commercial γ-Al_2O_3 samples fluorinated at 450/480°C show very similar TPD behaviour. As shown by PAS, the Brønsted centres are easily lost while the Lewis sites are unaffected. TPD conditions in the first run affect mainly the Brønsted sites and the remaining strong sites in highly fluorinated samples are mainly Lewis in nature.

The results of the characterisation of active centres are consistent with catalytic testing in model reactions, as shown in table 3. The catalytic behaviour of aerogel and xerogel is opposite: aerogel is active in dehydrochlorination of CCl_3CH_3, while the xerogel shows activity in isomerisation of 1-butene. It can be concluded that the highly fluorinated samples can be regarded as relatively strong Lewis acid catalysts, while the samples with

Table 3
Characteristics of acidic sites and catalytic activity in model reactions for aerogel and xerogel treated with CHF_3 at 350°C

	Aerogel	Xerogel
acidic sites		
type (PAS-pyridine)	Lewis + some Brønsted	Brønsted + some Lewis
strength (ammonia TPD)	high	lower
distribution (ammonia TPD)	narrow	broad
activity in		
dehydrochlorination of CCl_3CH_3 at 130°C	active	non-active
isomerisation of 1-butene at 165°C	non-active	active

the lower degree of fluorination exhibit Brønsted and Lewis acidity with a broad distribution of strengths with the maximum situated in the medium range.

3.3. Isomerisation of CHF_2CHF_2

Representative results are shown in figs. 4a and 4b for the active and non- (or less) active catalysts respectively. The courses of the isomerisation in the presence of highly fluorinated commercial γ-Al_2O_3 (samples C-H450 and C-F480 in fig. 4a) are very similar to the behaviour of the chromia catalyst [4]. The HF-treated catalyst is apparently more active at the beginning, but after 30 pulses the activity of the two is practically equal. Aerogel A-H350 catalyst shows a very similar reaction course but with lower conversion. Commercial γ-Al_2O_3 and xerogel, both fluorinated at 350°C, exhibit no activity at 400°C and only a small increase in activity at 450°C (fig. 4b). Very similar behaviour is exhibited by the A-F300 sample. In these, partly fluorinated samples, a considerable amount of unconverted oxide is still present and the remaining hydroxyl groups can easily rearrange the surface layer. The colour of all catalysts tested was dark grey or completely black after isomerisation, indicating strong coke formation due to destruction reactions of the haloethane with surface hydroxyl groups. Carbonisation is probably one of the main reasons for the observed gradual decrease in the activity of all catalysts as was also the case for chromia catalysts [4].

Noticeably different is the behaviour of the two aerogels, CHF_3-treated at 350 and 400°C. These catalysts are inactive at 400°C and slowly gain isomerisation activity at 450°C. When once "activated" catalysts are reused at

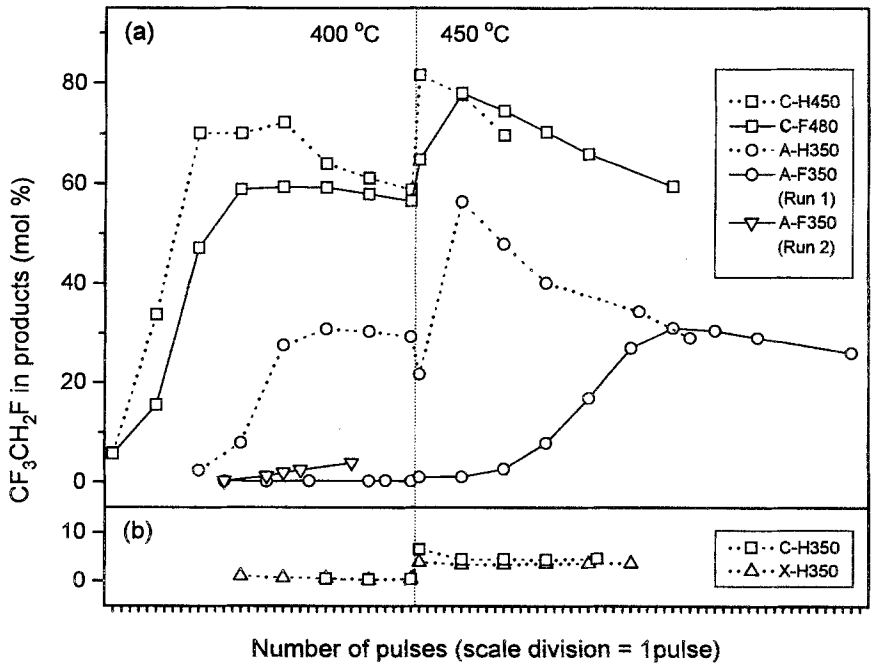

Fig. 4. Concentration of CF_3CH_2F in reaction products in dependence on the number of pulses for: (a) active and (b) less-active catalysts; catalysts fluorinated with: HF (dotted lines) or CHF_3 (solid lines); vertical dotted line represents the change in reaction temperature from 400 to 450°C.

400°C they are active practically from the beginning. Typical isomerisation behaviour is represented in fig. 4a for the A-F350 sample. The catalytic characteristics of the fresh, CHF_3-treated aerogels are therefore markedly different from the equivalent HF-treated samples. These differences between the two groups are somehow surprising, since, as discussed so far, both showed very similar surface properties. At the moment the reasons for these differences in initial catalytic activity are not clearly evident. Both the formation of slightly different acidic sites and the blocking of centres which have been already formed on the surface by halocarbon species can cause lower activity in the case of CHF_3-fluorinated samples.

Disregarding the discrepancies between aerogels, which seem to be related only to the initial stage of the reaction, it is evident that only highly fluorinated materials are catalytically, active in isomerisation of CHF_2CHF_2 (fig. 4a). All these materials are characterised by a well-defined TPD maximum at approximately 330°C indicating strong acid centres that are, according to PAS results, predominantly Lewis in nature. We can conclude that relatively strong Lewis acid catalysts are needed to perform the isomerisation. Partially fluorinated materials (fig. 4b) having a considerable amount of Brønsted acid centres show very low catalytic activity accompanied by decomposition of the gaseous reactant forming coke. For this reason it is very unlikely that conditioning with CHF_2CHF_2 to form a catalytically active material, as described from chromia [4], could be applicable to alumina materials.

Acknowledgement

This work was performed within the framework of a joint Slovene–German research project (1F1A6A). The authors are grateful to the International Büro, Forschungszentrum Jülich GmbH and to the Ministry of Science and Technology of the Republic of Slovenia for the financial support. The experimental contribution of K.-U. Niedersen and Dr. A. Hess is gratefully acknowledged.

References

[1] T. Skapin, J. Mater. Chem. 5 (1995) 1215.
[2] G.J. Moore and H.M. Massey, EP 0 365 296 A1 (1990).
[3] L.E. Manzer and V.N.M. Rao, US 4,902,838 (1990).
[4] E. Kemnitz and K.-U. Niedersen, J. Catal. 155 (1995) 283.
[5] A. Hess and E. Kemnitz, J. Catal. 149 (1994) 449.
[6] B. Sedej, Talanta 23 (1976) 335.
[7] B. Adamczyk, Diploma Thesis, Humboldt-University, Berlin, Germany (1995).
[8] G.B. McVicker, C.J. Kim and J.J. Eggert, J. Catal. 80 (1983) 315.
[9] R.I. Hegde and M.A. Barteau, J. Catal. 120 (1989) 387.
[10] E.C. DeCanio, J.W. Bruno, V.P. Nero and J.C. Edwards, J. Catal. 140 (1993) 84.
[11] P.O. Scokart, S.A. Selim, J.P. Damon and P.G. Rouxhet, J. Colloid Interf. Sci. 70 (1979) 209.
[12] K.S.W. Sing, D.H. Everett, R.A.W. Haul, L. Moscou, R.A. Pierotti, J. Rouquerol and T. Siemieniewska, Pure Appl. Chem. 57 (1985) 603.
[13] J. Thomson, G. Webb and J.M. Winfield, J. Chem. Soc. Chem. Commun. (1991) 323.
[14] T.H. Ballinger and J.T. Yates, J. Phys. Chem. 96 (1992) 1417.
[15] Z.X. Cheng and V. Ponec, Appl. Catal. A 118 (1994) 127.
[16] S.M. Maurer and E.I. Ko, Catal. Lett. 12 (1992) 231.